Local Activation Time Estimation in Fractionated Electrograms of Cardiac Mappings

Bahareh Abdi, Alle-Jan van der Veen, Natasja M.S. de Groot and, Richard C. Hendriks

Abstract— In this study, we propose a novel approach for estimation of local activation times (LATs) in fractionated electrograms. Using an electrophysiological tissue model, we first formulate the electrogram array as a convolution of transmembrane currents with a distance kernel. These currents are more local activities and less affected by the heterogeneity in the tissue compared to electrograms. We then deconvolve the distance kernel with the electrograms to reconstruct the transmembrane current. To stabilize the solution of this ill-posed deconvolution, we use spatio-temporal total variation as a regularization. This helps to preserve sharp spatial and temporal deflections in the currents that are of higher importance in LAT estimation. Finally, the maximum negative slope of the reconstructed transmembrane currents are used to estimate the LATs. Instrumental comparison to two reference approaches shows that the proposed approach performs better in estimating the LATs in fractionated electrograms.

I. INTRODUCTION

Cardiac activation maps (AMs) are important diagnostic tools that are broadly used to represent depolarization wave-front propagation patterns, used for many applications, e.g., to estimate the tissue conductivity, to analyze conduction disorders, and to guide the cardiologist through ablation therapies of atrial fibrillation. These maps are based on the local activation times (LATs) of the underlying cells. The most commonly used approach (from here on referred to as standard approach) in estimating the activation time of a normal unipolar epicardial electrogram as shown in Fig. 1(d), is to use the maximum negative slope of the electrogram [1]. However, as shown in Fig. 1(c), electrograms can be quite fractionated during atrial fibrillation specially in areas with conduction disorders. In these cases, the maximum negative slope may not coincide with the true LAT. This can make the estimation of LATs and its further analysis quite challenging.

Various approaches have been proposed to overcome the challenges in estimating the true activation time of a fraction-ated electrogram. Some approaches employ the electrogram's morphological features to provide a better estimation of LAT. This includes the annotation of the center of the mass of the atrial activity as the LAT [2] or matching the recorded elec-trogram with a library of template fractionated electrograms [3]. In some other methods, the global activation maps are formed by initially finding the delays between neighboring

Bahareh Abdi, Richard C. Hendriks, and Alle-Jan van der Veen are with Faculty of Electrical Engineering, Mathematics and Computer Science,Technical University of Delft, 2628 CD Delft, The Netherlands (e-mail:b.abdikivanani@tudelft.nl, r.c.hendriks@tudelft.nl, a.j.vanderveen@tudelft.nl)

Natasja M.S. de Groot is with the Department of Cardiology, Eras-mus University Medical Center,3062 PA Rotterdam,The Netherlands (e-mail:n.m.s.degroot@erasmusmc.nl)

electrograms and then finding a global activation map that fits these delays the best [4]. It has also been shown in some studies that spatial processing of the multi-electrode recordings can improve the performance of LATs estimation in fractionated electrograms. This can be done by annotating the maximum spatial gradient or the zero crossing of the surface Laplacian of the electrogram array as the LATs [5].

As previously demonstrated in some studies [6], [7], incorporating the electrophysiological model of the electri-cal propagation can improve the performance of the LAT estimation. According to these models, the electrogram is a weighted summation of the transmembrane currents gen-erated by the myocardial cells in its neighborhood. The weights depend inversely on the cells' distance from the electrode. The electrogram array can thus be formulated as a spatial convolution of the transmembrane currents and an appropriate distance kernel [6]. The deconvolution of the distance kernel with the electrogram array should therefore provide more local activities that are less affected by the heterogeneities in the tissue and can be used for a better estimation of activation times. Since there are more current sources in the tissue than the number of electrodes, this inverse problem of deconvolution is ill-posed. To avoid this problem, some earlier studies have simplified the problem by assuming a planar wave propagation with a constant velocity across the tissue [6]. The focus is then on the estimation of wave travel times from a source to the electrodes. Some other studies use data interpolation to increase the spatial resolution of electrograms. It is then followed by spatial filtering to enhance the local activities in each electrogram before the deconvolution [7].

In this study we propose a novel systematic approach for a better estimation of LATs in fractionated electrograms. The approach stabilizes the solution of the spatial decon-volution problem of transmembrane current estimation by employing spatio-temporal edge-preserving regularization. The approach effectively preserves the sharp spatio-temporal changes of the transmembrane currents that are of importance in activation time estimation. Moreover, we formulate the regularized deconvolution problem in a way that it can ben-efit from fast Fourier transformations and use the alternating direction method of multipliers (ADMM) [8] to accelerate the computations.

II. METHODS

A. Convolutive Electrogram Model

When the depolarization wave-front propagates through the tissue and the action potentials are triggered, each cell

acts as a current source, generating the so called transmembrane current. Since it is complicated and not practical to model all cells we employ source clamping by replacing each group of cells in the 3D tissue with a modeled cell in a 2D mono layer grid. We denote the transmembrane current of a modeled cell located at $\mathbf{x}_n$ and at the time sample t by $I_{\text{tm}}(\mathbf{x}_n, t)$, where $n \in 1, 2, .., N_c$ is the cell index and $N_c = r_c \times c_c$ is the total number of modeled cells or the elements of the grid with r_c rows and c_c columns. The electrogram $\Phi_m(t)$ is a record of changes in the electrical potential of the (many) cells in the electrode neighborhood, where $m \in 1, 2, ..., M$ is the electrode index. The electrogram can be formulated based on the transmembrane currents using

$$\Phi_m(t) = \frac{1}{4\pi\sigma_e} \sum_{n=1}^{N_c} \frac{I_{\text{tm}}(\mathbf{x}_n, t)}{r_{m,n}} \Delta x^2, \tag{1}$$

where Δx is the cell-to-cell distance on the assumed uniform grid. Assuming that the electrode array is also located on a two-dimensional grid parallel to the tissue surface at a height that equals z_0, the cell-to-electrode distance $r_{m,n}$ will be $r_{m,n} = \sqrt{\|\mathbf{y}_m - \mathbf{x}_n\|^2 + z_0^2}$, where $\mathbf{y}_m$ is the electrogram's location.

Eq. (1) can be expressed as a spatial convolution of transmembrane currents with the appropriate distance kernel $\mathbf{R}$. We first introduce matrix $\mathbf{I}(t)$ of size $r_c \times c_c$ as the transmembrane current map containing all per cell currents at time sample t. Note that in this paper *map* refers to the 2D data structures containing the discretized per cell or per electrode values of a signal at a single temporal sample. Likewise, matrix $\mathbf{\Phi}'(t)$ of size $r_c \times c_c$ is the full resolution electrogram map containing all per cell electrograms. The spatial convolutive model is then

$$\mathbf{\Phi}'(t) = c\,\mathbf{R} * \mathbf{I}(t), \tag{2}$$

where all the constants are collected in $c = \Delta x^2 / 4\pi\sigma_e$ which will be omitted in the subsequent analysis for simplification purposes. The matrix $\mathbf{R}$ has a limited support of size $(2b+1) \times (2b+1)$ and its element at the ith row and j^{th} column can be calculated as $[\mathbf{R}]_{i,j} = ((|i-b|\Delta x)^2 + (|j-b|\Delta x)^2 + z_0^2)^{-1/2}$.

To rewrite the convolution in Eq. (2) as a matrix-vector multiplication we first introduce vector $\mathbf{i} = [\text{vec}(\mathbf{I}(0)), \text{vec}(\mathbf{I}(1)), ..., \text{vec}(\mathbf{I}(T-1))]^T$ as the matrix containing all per cell currents at all time samples $t \in 0, 1, .., T-1$, where $\text{vec}(\cdot)$ stacks the columns of the argument matrix to form a vector. Likewise, $\mathbf{\phi}' = [\text{vec}(\mathbf{\Phi}'(0)), \text{vec}(\mathbf{\Phi}'(1)), ..., \text{vec}(\mathbf{\Phi}'(T-1))]$ contains all the resulting per cell electrograms. However, in clinically recorded data, we do not have access to electrograms recorded at all grid elements of the modeled tissue, but only to those with an electrode on top. Moreover, there can be some broken or faulty electrograms whose data cannot be used. To take this into account, instead of interpolating the unknown electrograms, we use a row selection matrix $\mathbf{S}$ to select the cells with available electrograms denoted by $\mathbf{\phi}$.
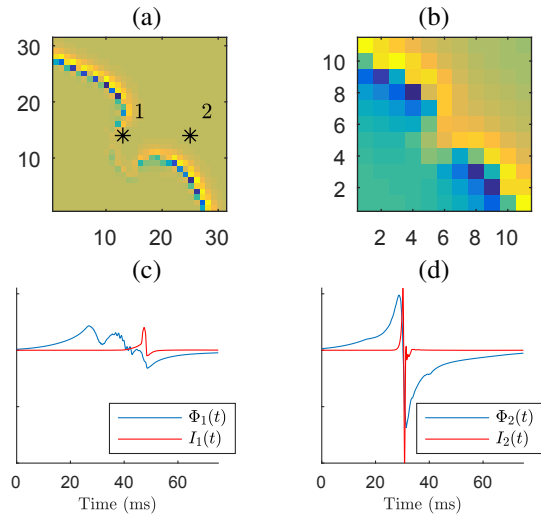

Fig. 1. The transmembrane current map (a) as well as the lower resolution electrogram map (b) of the same tissue at the same time instance. The simulated electrograms and the transmembrane currents at electrode location 1 and 2 denoted by *, are also shown in (c) and (d), respectively.

The matrix-vector multiplication model of the electrogram is then

$$\mathbf{\phi} = \mathbf{S}\tilde{\mathbf{R}}\mathbf{i}, \tag{3}$$

where matrix $\tilde{\mathbf{R}}$ implements the convolution in Eq. (2).

Fig. 1(a) shows an example of transmembrane current map at a single time sample on a 2D simulated tissue. The conductivity map and the complete activation map through one atrial beat of the same tissue are shown in the first column of Fig. 2, more details on the simulation can be found in Section III. In the simulated tissue, there is a conduction block in the middle, where the wavefront is delayed. Fig. 1(b) shows the low resolution electrogram map of the same data recorded by an array whose inter-electrode distances are 3 times the cell-to-cell distances. As can be seen, the wavefront in the transmembrane current map is more distinct and the borders of the block are more clear.

B. Transmembrane Current Estimation

Our aim in this section is to estimate the unknown transmembrane currents $\mathbf{i}$ based on the recorded electrograms $\mathbf{\phi}$. Since the number of measured electrograms M is less than the number of modeled cells N_c, a cost function that employs only a data-fitting term is highly ill-posed and results in an unstable solution. Adding a regularization function that employs some prior knowledge on the data helps to stabilize the solution and penalizes impractical solutions.

In this paper, we propose the application of the edge preserving spatio-temporal total variation (TV) regularization due to the following criteria: (1) It does not employ any specific assumption that may only be applicable to homogeneous tissues, like assuming a stereotype transmembrane current for all cells, or planar wave propagation with constant velocity, (2) it preserves the main features of the transmembrane currents that are of higher importance for LAT estimation which, as demonstrated in previous studies [5], are fast spatial and temporal changes, and (3) it can be solved using

computationally efficient fast approaches and is practical for large amount of clinical data [9]. The TV regularization function is given by

$$\psi(\mathbf{D}\mathbf{i}) = \sum_{i=1}^{N_cT} \sqrt{|[\mathbf{D}_v\mathbf{i}]_i|^2 + |[\mathbf{D}_h\mathbf{i}]_i|^2 + k|[\mathbf{D}_t\mathbf{i}]_i|^2} \qquad (4)$$

where $\mathbf{D}_v$, $\mathbf{D}_h$, and $\mathbf{D}_t$ of size $N_cT \times N_cT$ are the first order vertical, horizontal, and temporal forward difference operators respectively, and k properly scales time derivatives with respect to spatial derivatives. We define operator $\mathbf{D} := [\mathbf{D}_v^T, \mathbf{D}_h^T, k\mathbf{D}_t^T]^T$ to denote the concatenation of the three operators. The final regularized objective function for estimation of $\mathbf{i}$ is then given by

$$\frac{1}{2}\|\boldsymbol{\phi} - \mathbf{S}\tilde{\mathbf{R}}\mathbf{i}\|_2^2 + \lambda\,\psi(\mathbf{D}\mathbf{i}), \qquad (5)$$

where λ is the regularization parameter. The regularization term is used to obtain solutions where edges and disconti-nuities are preserved.

C. Implementation

A variety of numerical approaches can be implemented to solve the optimization problem in Eq. (5), among which we opt for ADMM. This algorithm solves a convex optimization problem by breaking it into smaller problems which are sim-pler to solve. Furthermore, ADMM has a fast convergence rate to a reasonable precision in practice. In this study we employ the ADMM framework proposed in [10] to solve the optimization problem in Eq. (5). In this approach two auxiliary variables $\mathbf{u}_1 = \tilde{\mathbf{R}}\mathbf{i}$ and $\mathbf{u}_2 = \mathbf{D}\mathbf{i}$ are introduced to separate the distance kernel and the selection matrix. The new augmented Lagrangian (AL) function is

$$\mathcal{L}(\mathbf{i}, \mathbf{u}_1, \mathbf{u}_2, \mathbf{d}_1, \mathbf{d}_2) = \frac{1}{2}\|\boldsymbol{\phi} - \mathbf{S}\mathbf{u}_1\|_2^2 + \frac{\mu_1}{2}\|\mathbf{u}_1 - \tilde{\mathbf{R}}\mathbf{i} - \mathbf{d}_1\|_2^2$$
$$+ \lambda\,\psi(\mathbf{u}_2) + \frac{\mu_2}{2}\|\mathbf{u}_2 - \mathbf{D}\mathbf{i} - \mathbf{d}_2\|_2^2, \qquad (6)$$

where μ_1 and μ_2 are AL penalty parameters, and $\mathbf{d}_1$ and $\mathbf{d}_2$ are Lagrange multipliers. We then solve the optimiza-tion problem by alternatively estimating one variable (by minimizing its corresponding objective function) at each step, while the other parameters are fixed. This procedure is repeated until some stopping criteria are met. The fast con-vergence speed of the proposed approach arises firstly from the employed ADMM approach and secondly from replacing all large matrix multiplications (convolutions and derivatives) in each step with discrete Fourier transforms (DFTs) by assuming periodic boundary conditions for convolution.

D. Activation Time Estimation

The per cell estimated transmembrane currents are by definition more local activities than the electrograms, and less affected by heterogeneities in the conductivities of their neighboring cells. Therefore, they can be used for a more accurate estimation of the activation times compared to electrograms. For each electrode, we use the maximum negative slope of the transmembrane current (as presented for electrograms) of the closest cell on the grid as its estimated activation time.
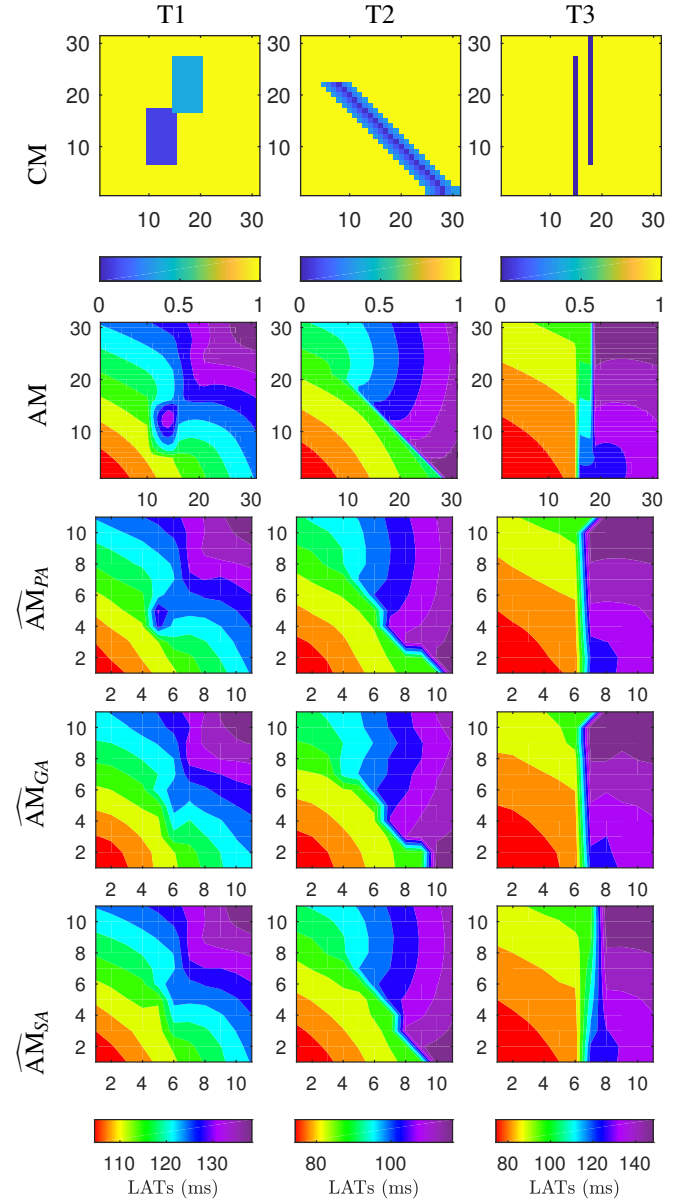

Fig. 2. The first row represents the normalized isotropic conductivity map of three different types of 2D simulated tissues. The second row shows the true activation maps, in all cases the tissue is stimulated from the left bottom corner. The third to fifth row represent the estimated activation maps using the proposed approach, the gradient based approach, and the standard approach, respectively.

III. RESULTS

We do not have access to ground truth LATs in clinically recorded electrograms. To demonstrate the performance of the model and to compare its results with other approaches, we therefore use simulated 2D tissues. The monodomain action potential propagation model [11] with the Courte-manche atrial cellular model [12] is employed to simulate the wavefront propagation in 2D atrial tissue of size 129×129 cells. The modeled cell size is $\Delta x = 2/3\,\text{mm}$ which is one third of the inter-electrode distances used in our clinical measurements. Three electrical conductivity maps with different patterns of blocks and slow conductions are

used to simulate electrograms and to insure generation of fractionated electrograms with different patterns. The maps are denoted by T1, T2 and T3 and are shown in the first row of Fig. 2. The isotropic tissues, are stimulated with a stimulation current injected to the cell at the left bottom of the tissue. The initial sampling period for modeling propagation is $T_s = 0.02$ ms, but the final electrograms are down-sampled to have a sampling period of $T_s = 0.2$ ms. A more detailed description of the simulation steps and parameters can be found in [13]. The employed conductivity maps and the resulting true activation maps are shown in the first and second row of Fig. 2. Notice that the plots only show the 31×31 central cells where the electrode array of size 11×11 electrodes is positioned. The inner-electrode distance is $3\Delta x$. The size of the distance kernel for generating the data is $2b + 1 = 129\Delta x$ (the same size as the grid), but it was reduced to $2b + 1 = 11\Delta x$ in the inverse problem to reduce computational complexity.

The proposed approach (from here on referred to as PA) is employed on the simulated electrograms. First the atrial activities of all modeled cells in $\mathbf{i}$, are estimated using Eq. (6) and then the LATs are estimated. The results are demonstrated in the third row of Fig. 2. To evaluate the performance, we use two other references: the gradient based approach (GA) and the standard approach (SA), implemented based on the methods presented in [5] and [1], respectively. GA annotates the maximum of the spatial gradient of the electrogram array as the estimated activation time, whereas SA annotates the maximum negative temporal slope of the electrogram. The results of these two approaches are demonstrated in the fourth and fifth row of Fig. 2, respectively. Moreover, Table I shows the root mean square error (RMSE) in ms between the true LATs and the estimated LATs of fractionated electrograms for each tissue using the proposed and reference approaches. The fractionated electrograms were selected as those having multiple deflections (only deflections with amplitudes higher than 30% of the maximum negative slope were considered). This resulted in selecting 15, 17 and 26 fractionated electrograms from T1, T2, and T3 respectively.

As can be seen in Fig. 2 and Table I, our approach provides a better LAT estimation than the standard approach. While the gradient based approach and proposed approach preserve the sharp changes in the activation times, the standard approach provides LATs that change (too) smoothly across the map where the blocks in the middle might be missed. On the other hand, the gradient based approach provides non smooth results in smooth areas of the tissue which can complicate the further analysis of activation map isochrones by a cardiologist. In tissue T3, the blocks force the wave to follow a zigzag path which results in highly fractionated electrograms and all approaches perform comparably bad providing large errors in LATs estimation.

IV. CONCLUSION

In this paper we proposed a new approach for estimation of the activation times in electrograms employing the electro-

	PA	GA	SA
T1	3.1	8.2	8.7
T2	9.2	11.5	13.2
T3	24.1	24.7	33.8

gram convolutive model. The approach uses spatio-temporal TV regularization to stabilize the ill-posed deconvolution problem and to preserve the sharp deflections in the data. The results show that the approach can improve the performance of LATs estimation in fractionated electrograms. The TV regularization preserves the sharp deflection in the estimated per cell transmembrane currents in the spatial and temporal domain which coincides with the true activation time of the cell. This can improve the performance of automatic approaches that aim to detect blocks and discontinuities in the tissue.

REFERENCES

[1] C. D. Cantwell, C. H. Roney, F. S. Ng, J. H. Siggers, S. Sherwin, and N. S. Peters, "Techniques for automated local activation time annotation and conduction velocity estimation in cardiac mapping," *Computers in biology and medicine*, vol. 65, pp. 229–242, 2015.

[2] L. Sandrini, L. Faes, F. Ravelli, R. Antolini, and G. Nollo, "Morphology-based measurement of activation time in human atrial fibrillation," in *Computers in Cardiology*. IEEE, 2002, pp. 593–596.

[3] R. P. Houben, N. M. de Groot, F. W. Lindemans, and M. A. Allessie, "Automatic mapping of human atrial fibrillation by template matching," *Heart Rhythm*, vol. 3, no. 10, pp. 1221–1228, 2006.

[4] R. Dubois, S. Labarthe, Y. Coudière, M. Hocini, and M. Haïssaguerre, "Global and directional activation maps for cardiac mapping in electrophysiology," in *Computing in Cardiology (CinC), 2012*. IEEE, 2012, pp. 349–352.

[5] B. B. Punske, Q. Ni, R. L. Lux, R. S. MacLeod, P. R. Ershler, T. J. Dustman, M. J. Allison, and B. Taccardi, "Spatial methods of epicardial activation time determination in normal hearts," *Annals of biomedical engineering*, vol. 31, no. 7, pp. 781–792, 2003.

[6] W. S. Ellis, S. J. Eisenberg, D. M. Auslander, M. W. Dae, A. Zakhor, and M. D. Lesh, "Deconvolution: A novel signal processing approach for determining activation time from fractionated electrograms and detecting infarcted tissue," *Circulation*, vol. 94, no. 10, pp. 2633–2640, 1996.

[7] I. Chouvarda, N. Maglaveras, J. M. de Bakker, F. J. van Capelle, and C. Pappas, "Deconvolution and wavelet-based methods for membrane current estimation from simulated fractionated electrograms," *IEEE transactions on biomedical engineering*, vol. 48, no. 3, pp. 294–301, 2001.

[8] S. Boyd, N. Parikh, E. Chu, B. Peleato, J. Eckstein *et al.*, "Distributed optimization and statistical learning via the alternating direction method of multipliers," *Foundations and Trends® in Machine learning*, vol. 3, no. 1, pp. 1–122, 2011.

[9] W. Lu, J. Duan, Z. Qiu, Z. Pan, R. W. Liu, and L. Bai, "Implementation of high-order variational models made easy for image processing," *Mathematical Methods in the Applied Sciences*, vol. 39, no. 14, pp. 4208–4233, 2016.

[10] A. Matakos, S. Ramani, and J. A. Fessler, "Accelerated edge-preserving image restoration without boundary artifacts," *IEEE transactions on image processing*, vol. 22, no. 5, pp. 2019–2029, 2013.

[11] R. Plonsey and R. C. Barr, *Bioelectricity: a quantitative approach*. Springer Science & Business Media, 2007.

[12] M. Courtemanche, R. J. Ramirez, and S. Nattel, "Ionic mechanisms underlying human atrial action potential properties: insights from a mathematical model," *American Journal of Physiology-Heart and Circulatory Physiology*, vol. 275, no. 1, pp. H301–H321, 1998.

[13] B. Abdi, R. C. Hendriks, A.-J. van der Veen, and N. M. de Groot, "A compact matrix model for atrial electrograms for tissue conductivity estimation," *Computers in biology and medicine*, vol. 107, pp. 284–291, 2019.